HHS Public Access

Author manuscript

Cancer Gene Ther. Author manuscript; available in PMC 2016 July 14.

Published in final edited form as:

Cancer Gene Ther. 2010 December ; 17(12): 855–863. doi:10.1038/cgt.2010.42.

Blood outgrowth endothelial cell-based systemic delivery of antiangiogenic gene therapy for solid tumors

Vidya Bodempudi[1], **John R. Ohlfest**[2], **Kaoru Terai**[1], **Edward A. Zamora**[2], **Rachel Isaksson Vogel**[3], **Kalpna Gupta**[1], **Robert P. Hebbel**[1], and **Arkadiusz Z. Dudek**[1]

[1]Vascular Biology Center and Department of Medicine, Division of Hematology, Oncology and Transplantation, University of Minnesota, Minneapolis, MN, USA, 55455

[2]Department of Pediatrics, University of Minnesota Medical School, Minneapolis, MN, USA, 55455

[3]Biostatistics and Bioinformatics, University of Minnesota Masonic Cancer Center, Minneapolis, MN, USA, 55455

Abstract

Endothelial cells and endothelial cell precursors encoding a therapeutic gene have induced antitumor responses in preclinical models. Culture of peripheral blood provides a rich supply of autologous, highly proliferative endothelial cells, also referred to as blood outgrowth endothelial cells (BOECs). The aim of this study was to evaluate a novel antiangiogenic strategy using BOECs expressing fms-like tyrosine kinase-1 (sFlt1) and/or angiostatin-endostatin (AE) fusion protein. Conditioned medium from BOECs expressing sFlt1 or AE suppressed *in vitro* growth of pulmonary vein endothelial cells by 70% compared to conditioned medium from non-transduced BOEC controls. RT-PCR analysis indicated that systemically administered BOECs proliferated in tumor tissue relative to other organs in C3TAG mice with spontaneous mammary tumors. Tumor volume was reduced by half in C3TAG mice and in mice bearing established lung or pancreatic tumors in response to treatment with sFlt1-BOECs, AE-BOECs or their combination. Studies of tumor vascular density confirmed that angiogenic inhibition contributed to slowed tumor growth. In an orthotopic model of glioma, the median survival of mice treated with sFlt1-BOECs was double that of mice receiving no BOEC treatment (p=0.0130). These results indicate that further research is warranted to develop BOECs for clinical application.

Corresponding Author: Arkadiusz Dudek, MD, PhD, Division of Hematology, Oncology and Transplantation, University of Minnesota, 420 Delaware Street SE, MMC 480, Minneapolis, MN 55455, Tel: 612 624-0123/ fax: 612 625-6919, dudek002@umn.edu.

Disclosure of Potential Conflicts of Interest

The University of Minnesota and RPH own a patent on the BOEC culture technology employed in this research, but there is no current financial interest.

Financial disclosure: We thank The Susan G. Komen Breast Cancer Foundation (Grant # BCTR86006) (AZD) for supporting this research. This work was also supported by grants from the NIH; HL-55552 (RPH), CA109582 (KG), NS055738-01A2 (JRO), and the Dana Foundation (JRO).

Keywords

Blood outgrowth endothelial cells; cancer gene therapy; sFlt1; angiostatin-endostatin fusion protein

Introduction

Neovascularization is essential for tumor growth and metastasis. (1) Recent studies suggest that circulating endothelial progenitor cells travel through the circulation to sites of ongoing neovascularization and, once there or in circulation, differentiate into mature endothelial cells which then assist in new blood vessel formation in a process consistent with postnatal vasculogenesis. (2) *Ex vivo* cultures of human peripheral blood mononuclear cells can be used to create a population of blood outgrowth endothelial cells (BOECs). BOECs are not endothelial progenitor cells (EPC), as they are mature differentiated endothelial cells that are the progeny of a circulating, marrow-derived, transplantable, true EPC. (3) As a cellular vehicle for gene delivery, autologous BOECs have several advantages over other cell types, including low immunogenicity, ease of collection from the peripheral blood, ease of expansion, stability in cell culture and ease of genetic manipulation. Indeed, a 10^{18}-fold expansion of BOECs can be achieved from only 50 to 100 ml of blood. (3) Moreover, these expanded BOECs maintain their phenotype and are amenable to genetic engineering as we and others have demonstrated. (4)

Previous work has shown that BOECs migrate through the circulatory system into the vascular bed of tumors in mice; however, the distribution of BOECs in tumor tissue and other organs was determined for only 3 days following BOEC infusion. (5) BOECs engineered to express endostatin are capable of secreting endostatin in the tumor microenvironment *in vivo* on a continuous basis, resulting in decreased tumor vascularization and tumor volume in mice bearing subcutaneously established Lewis lung tumors. (5) Based on these encouraging results, the next step to developing this technology was to assess the antitumor activity of antiangiogenic gene therapy with different gene products and in different tumor models, including ones thought to better represent human disease, such as spontaneous tumor models. In the present study, a novel strategy was pursued utilizing BOECs transduced using a retroviral vector to express the potent angiogenic inhibitors, soluble fms-like tyrosine kinase-1 (sFlt1) or angiostatin-endostatin (AE) fusion protein. (6) These angiogenic inhibitors antagonize distinct signaling networks involved in neovascularization, and therefore their combination could result in enhanced antitumor activity. BOECs expressing sFlt1 or AE were systemically delivered to mice, alone and in combination, to evaluate their effects on primary tumor growth, metastasis and survival in subcutaneous models of lung and pancreatic cancer, a model of spontaneous breast cancer metastasis, and an induced orthotopic model of glioma, respectively. In addition, the in vivo fate of systemically infused BOECs was monitored over a longer period of time compared to previous studies.

Materials and Methods

Cell culture

Murine Lewis lung carcinoma cells and human pancreatic cancer S2VP10 cells were maintained in Dulbecco's modified Eagle's medium (DMEM) supplemented with 10% fetal bovine serum (FBS), 100 U/ml of penicillin, and 100 μg/ml of streptomycin. Murine pulmonary vein endothelial cells (PVECs) and murine BOECs were grown and maintained using EGM-2 Bullet Kit medium (Clontech Laboratories, Inc) supplemented with 10% FBS and 0.15 g/liter dibutyryl cyclic-AMP. (7) Human umbilical vein endothelial cells (HUVEC) and human BOECs were grown and propagated in EGM-2 Bullet Kit medium supplemented with 10% FBS.

Construction of retroviral vector

Four retroviral vectors were constructed for the purposes of transfecting BOECs with the AE fusion protein, murine sFlt1, human sFlt1, and DsRed. The IRES DsRed cassette, consisting of 1959-base pairs (bp), was cut from the pIRES-DsRed-Express vector (Clontech) with XhoI and NotI and cloned into the retroviral expression vector, PLNCX2. This vector was named PLNCX2-DsRed. Subsequently, a 2012-bp fragment expressing the AE fusion gene (6) and a 1012-bp DNA fragment containing sFlt1 were cloned upstream of IRES in the PLNCX2-DsRed vector (Figure 1). Human sFlt1 (hsFlt) cDNA was obtained by PCR amplification of human placenta Quick-Clone cDNA (Clontech Laboratories, Inc). Quick-Clone cDNA (1 ng) was amplified using the forward primer 5′-GCTCACCATGGTCAGCTA-3′ and reverse primer 5′-CTGCTATCATCTCCGAACTC-3′ at a final concentration of 0.4 μmol, using DNA polymerase, dNTP and PCR buffer according to the manufacturer's instructions (Invitrogen). PCR conditions were as follows: 94°C for 5min followed by 40 cycles of 94°C for 15 sec, 55°C for 1 min, 72°C for 30sec, and 72°C for 10 min. The resulting PCR product of 2.2 kb was subcloned into the PCR-TOPO TA cloning vector according the manufacture's protocol (Invitrogen). The insertion of sFlt1 cDNA was confirmed by restriction digestion and sequencing. A 2.2 kb band was cut from PCR-TOPO TA vector with EcoRI and cloned into an EcoRI site upstream of IRES-DsRed in the PLNCX2-DsRed vector.

Plasmid DNA encoding PLNCX2-DsRed, PLNCX2-AE, PLNCX2-hsFlt1 (containing human sFlt1) and PLNCX2-msFlt (containing mouse sFlt1) vectors (Figure 1) were transfected into the virus-producing cell line, RetroPack PT67 (Clontech Laboratories), using Fugene6 according to the manufacturer's instructions (Roche Molecular Biochem). The stable cell line containing each of the 4 plasmids was then established by Neomycin selection for 3 to 4 weeks. Conditioned medium from PT67/DsRed was collected 48 hrs later and filtered through a 0.45μm cellulose acetate filter and stored at −80°C. Similarly, virus containing AE, hsFlt1 and msFlt1 was collected from the supernatant of PT67/AE, PT67/hsFlt1 and PT67/msFlt1, respectively.

Generation of stable transduced cell lines

BOECs at 60–70% confluence were transduced with each of the 4 vectors, respectively, by exposing cells to conditioned medium containing viral particles supplemented with 8μg/ml

of polybrene and 8μg/ml chondroitin sulfate C (Sigma-Aldrich Inc) for 24 hrs at 37°C followed by incubation in fresh BOEC medium. This step was repeated 4–5 times to increase the number of infected BOECs. Cells that were positive for the specific gene transfer were sorted using fluorescence-activated cell sorting (FACS). Sorted cells were maintained with complete medium containing 0.15mg/ml of G418 for selection of pure populations of transgene-positive cells.

Detection of transgene products and BOEC phenotype

Levels of endostatin, hsFlt-1(human) and msFlt (mouse) in BOEC culture supernatant and mouse plasma fractions were determined by using murine endostatin and Flt1 ELISA kits (Chemicon International and R&D Systems, respectively). ELISA was performed according to the manufacturer's instruction. Cells only transfected with DsRed served as a control for the ELISA.

Endothelial phenotype for each of the transfected BOECs was determined by morphology and expression of the endothelial markers flt-1, VE-cadherin, and CD31. Expression of markers for monocytes (CD14) and leukocyte common antigen (CD45) were used as negative controls.

Cell proliferation assay

Conditioned medium was collected from flasks containing AE-BOECs, hsFlt-BOECs, msFlt-BOECs, or Dsred-BOECs. Medium was filtered through a 0.45 μm filter unit, and aliquots were stored at −70°C for further use. PVECs were seeded in 96-well plates precoated with 1% gelatin at a density of 3×10^3 cells per well. Thawed conditioned medium supplemented with 0.15 g/liter dibutyryl cAMP and 50 ng/ml of basic fibroblast growth factor was added to the 6 wells per group. Positive control wells had PVECs with basal medium supplemented with dibutyryl cAMP and FGF. PVEC proliferation was determined at 24hrs, 48hrs and 72 hrs by tetrazolium salt WST-1 proliferation assay (Roche Biochem) according to the manufacturer's protocol. For hsFlt-BOECs, the proliferation assay was performed on both HUVECs and PVECs.

BOEC detection by real-time PCR in mice with spontaneous mammary carcinoma

Genomic DNA was isolated from different tissues using the DNeasy Tissue kit (Qiagen) according to the manufacturer's protocol. Real-time quantitative PCR was performed using an ICycler (Bio-Rad laboratories) to detect Y chromosome-specific DNA sequences as an indicator of male mBOECs in different mouse organs. The primers sequences designed for the sex-determining region Y (SRY) gene located on Y chromosome were as follows: sense primer 5′ GTC CCG TGG TGA GAG GCA CAA GT 3′, antisense primer 5′GCA GCT CTA CTC CAG TCT TGC C 3′ and probe 5′ TTT CTC TCT GTG TAA GAT CTT CAA TC – FAM-3′. Taqman rodent GAPDH control reagents containing universal primers (Applied Biosystems) were used as internal controls. Each real-time PCR reaction contained 500 ng of genomic DNA, 200nM of each primer, 150 nM of probe and 1X of iQ supermix (Bio-Rad). The PCR program consisted of denaturation at 95°C for 5 min followed by 60 cycles of 2-step PCR (95°C for 30s and 60°C for 30s). The modified cycle threshold (Ct) value was calculated by dividing the Ct for the SRY gene with that of GAPDH. The percentage of male

cells in each mouse organ was calculated based on the standard curve. The standard curve was obtained from the modified Ct value of the mouse genomic DNA obtained by mixing different percentages of male DNA with female DNA.

Tumor volume and metastases in mice with spontaneous mammary carcinoma

C3(1)SV40 TAG transgenic (C3TAG) mice. Female transgenic mice carrying a rat C3(1) simian virus 40 large tumor antigen (C3TAG) fusion gene develop highly invasive breast tumors and show the evolutionary spectrum of human infiltrating ductal carcinoma. (8) These mice develop ductal epithelial atypia at 8 weeks, progression to intra-epithelial neoplasia at 12 weeks (resembling human ductal carcinoma in situ), and invasive carcinoma and grossly palpable tumors at 16 weeks. By 6 months of age, all of the female mice die because of universal development of multifocal mammary adenocarcinomas. Breeder pairs of C3TAG mice on FVB/N strain were obtained from National Cancer Institute, Frederick, MD. Mice were bred and genotyped as described. (8) A total of 20 female mice were divided into two groups receiving murine BOECs (derived from FVB/N background mice to avoid immunologic rejection as would be the case for human BOECs) either transduced with DsRed (n=15) or msFlt1 (n=5). Ten- to 11-week-old mice were injected through the tail vein with a dose of 500,000 DsRed-mBOECs or msFlt1-mBOECs every other day for a total of three injections. All of the injected mBOECs were collected from male mice. Mice receiving DsRed-mBOEC injections were euthanized on days 0, 9 and 15 (n=5 per time point) for analysis of tumors size and metastases. Mice injected with msFlt1-mBOECs were sacrificed on day 9 (n=5). This experiment was performed twice independently, with analyses performed on 15 mice injected with DsRed-mBOECs and 5 mice injected with msFlt1-mBOECs. Tumor volumes were calculated as length × $width^2/2$. Following tumor measurements, tumors and other organs from the 30 mice receiving DsRed-mBOECs were analyzed for the presence of Y chromosome-specific DNA sequences (SRY gene) by quantitative RT-PCR as described above.

Tumor size in mice with subcutaneously established lung and pancreatic carcinomas

Eighty NOD/SCID mice were purchased from Jackson Laboratory (Bar Harbor, ME 04609 USA). Six-week-old mice were injected in the tail vein with anti-asialo GM1 antibody (Wako, Richmond, VA, USA) in order to eliminate natural killer cell activity in this mouse strain (9), which could affect *in vivo* survival of human BOECs. Mice were injected subcutaneously in the back with either Lewis lung cells (10,000 cells in 50 μl Matrigel) or S2VP10 cells (50,000 cells in 50 μl Matrigel). Three days after tumor cell implantation, mice were divided into groups of 10 and injected intravenously every other day for a total of three injections with either DsRed-hBOECs (Control), AE-hBOECs, hsFlt1-hBOECs, or a combination of AE-hBOECs and hsFlt1-hBOECs. Each dose consisted of 500,000 human BOECs per injection. After the last (third) BOEC injection, tumors were measured with calipers in two dimensions every other day for the duration of the experiment. Tumor volume was calculated using the formula for a sphere: length × $width^2/2$.

Detection of serum endostatin in Lewis lung carcinoma model

Mice implanted with Lewis lung carcinoma cells in the above experiment were used for measurement of murine endostatin. Serum samples were collected at the time of animal

sacrifice, and protein levels were measured with a murine endostatin ELISA kit (Chemicon International).

Quantification of tumor blood vessel density

CD31-stained tumor sections were quantified to assess microvessel density. Tumor microvessels were counted in sections after staining with antibodies specific to CD31 according to methods described previously. (5) Briefly, areas containing the highest number of capillaries were identified by scanning the tumor sections at low power (40×). After the areas of high vascular density were identified, the number of microvessels was assessed by counting microvessels in random 0.0321-mm^2 fields taken of each section at 200× magnification. Based on the criteria described by Weidner et al. (10) observation of a vessel lumen was not required.

Survival of mice with oncogene-induced glioma

The method employed to induce brain tumors was described previously. (11) Briefly, gliomas were induced in 1-day-old C57BL/6 mice in the right ventricle via co-transfection of plasmid DNA/polyethylenimine complexes encoding SV40-LgT, hyperactive human NRAS, and firefly luciferase (FLuc) with the Sleeping Beauty transposase gene. The injection into the right cerebral ventricle was performed with a 30 gauge hypodermic needle (12.5 bevel, Hamilton Company) attached to a micropump (Stoelting). Within 48 hours, mice were imaged to confirm luciferase expression. Three weeks after implantation, brain tumors in mice were verified with the IVIS 100 in vivo bioimaging system (Alameda, CA). Twenty-seven tumor-bearing mice were divided into three groups of mice receiving no treatment (n=10), wild-type murine BOECs (n=7), or murine BOECs encoding hsFlt1 (n=10). BOECs (500,000 cells) were injected through the tail vein every other day for a total of three injections. In this experiment murine BOECs cultured from C57BL/6 mice were used to avoid rejection as would occur if human BOECs were used in this immunocompetent mouse model. Animals were euthanized at the moribund state, when they could not reach food and water.

Statistical methods

ANOVA and t-tests were performed as appropriate to test for differences between control and experimental groups. Means ± standard errors are reported unless otherwise noted. Comparison of the number of metastatic tumors between treatment groups was done using Poisson regression. The natural log transformation was used for analyses involving tumor volumes, and the Cox Method was used to calculate means and confidence intervals on the original scale. (12) A general linear mixed model with a random intercept for each mouse and fixed effects for time and treatment was used for the longitudinal lung and pancreatic tumor volume measurements. A similar model, with a random intercept for each mouse and a fixed effect for treatment or location, was fit for the distribution of BOECs and vascular density data. Kaplan-Meier survival curves and median survival was determined for each of the treatment groups. (13) Survival was compared between treatment groups using the log rank test. A p-value of less than 0.05 was considered statistically significant. All analyses were carried out in SAS Version 9.2 (SAS Institute, Inc., Cary, NC).

Results

Phenotype and transgene expression of engineered BOECs

Human and mouse BOECs were stably transduced with either the AE fusion protein, mouse sFlt1 (msFlt1), human sFlt1 (hsFlt1), or DsRed. Engineered BOECs retained the morphology and surface markers of endothelial cells (data not shown). Transgene expression of endostatin (in BOECs with the AE fusion gene), msFlt1, and hsFlt1 (in BOECs transduced with the murine or human SFlt1 gene) was verified with the respective ELISA test. Supernatant collected in quinticates (n=5) from 48-hour cultures of BOECs (1×10^6 cells) encoding AE, msFlt1 or hsFlt1 contained, respectively, 504±19 ng/ml of endostatin, 399±3 ng/ml of msFlt1, and 406±9 ng/ml of hsFlt1. By comparison, only a negligible fraction of these proteins was detected in supernatant collected from DsRed-BOECs and mouse plasma fractions.

Endothelial cell proliferation in cultures containing BOEC supernatant

To evaluate the biological function of endostatin and Flt-1, a proliferation assay was performed by growing murine pulmonary vein endothelial cells (PVECs) in supernatant collected from AE-BOECs and msFlt1-BOECs. Compared to control DsRed-BOECs, a 70% decrease in the growth of PVECs was observed after 48 hrs of culture (Figure 2; p-value for difference <0.0001). HsFlt-BOECs were capable of inhibiting both PVECs and human umbilical vein endothelial cells (HUVECs) at comparable levels as that seen for AE-BOECs and msFlt1-BOECs (data not shown). Supernatant from murine BOECs encoding AE did not inhibit HUVEC proliferation (data not shown).

In vivo distribution of BOECs in the tumor, liver, spleen, and kidney

Male mouse DsRed-mBOECs were injected into the tail vein of 30 female C3TAG mice with spontaneous mammary tumors. To assess the *in vivo* distribution of mBOECs, tumors and organs were harvested on days 0, 9, and 15 after BOEC injection for quantitative RT-PCR analysis of Y chromosome-specific DNA sequences (Figure 3). Within the first 3 hrs of injection, BOECs were identified in the liver, kidney, spleen, and tumor, with the majority of cells trapped in the lungs. By day 9, however, the number of cells in lung tissue was significantly lower than that seen in the tumor (p=0.0001). By day 15, the number of BOECs in tumor tissue increased significantly compared to day 9 (p<0.0001), whereas the number of BOECs decreased in the liver (p=0.0042). The number of BOECs decreased in the lungs, and kidneys, and remained stable in spleen from 3 hours until day 15, though this observation did not reach statistical significance (p=0.2152, 0.1007, and 0.5529, respectively).

Metastasis in a spontaneous mammary tumor model

Female C3TAG mice with spontaneous mammary tumors were sacrificed on days 0, 9, and 15 after completing a series of injections with DsRed-mBOECs or msFlt1-mBOECs. In mice injected with DsRed-mBOECs, tumor size increased gradually from day 0 to 15 (data not shown). In contrast, mice receiving msFlt1-mBOECs had smaller primary and fewer metastatic tumors, which were seen mostly in lung, on day 9 compared to control mice

receiving DsRed-mBOECs (p=0.0613; Figure 4A–B). Further, the average tumor volume for all mice receiving msFlt1-mBOECs was reduced by 65% by day 9 compared to mice receiving DsRed-mBOECs (msFlt-mBOECs: 35.4mm^3, 95% CI 13.4–93.4 mm^3; DsRed-mBOECs: 80.1 mm^3, 95% CI: 41.8–153.4 mm^3; p=0.0095; Figure 4C).

Subcutaneous growth and vascularization of lung and pancreatic tumors

Mice were implanted with subcutaneous Lewis lung carcinoma cells. On days 4, 6, and 8 after tumor implantation, mice were injected with either DsRed-hBOECs, AE-hBOECs, hsFlt1-hBOECs or AE+hsFlt1-hBOECs (500,000 cells/injection). Immediately after the last hBOEC injection, the average tumor volume of Lewis lung tumors was 86.4±3.5 mm^3. Tumor growth in mice receiving combination AE+hsFlt1-hBOECs was significantly slower than all other groups (p≤0.001; Figure 5A). The average tumor volume in mice treated with control DsRed-hBOECs or AE+msFlt1-hBOECs on day 13 was 978±60 mm^3 and 509 ±105mm^3, respectively. Neither treatment with AE-hBOECs alone nor hsFlt1-hBOECs alone resulted in significantly different tumor growth compared to controls (p=0.5394 and p=0.2269 respectively). In addition, vascular density in Lewis lung tumors was lower in mice injected with BOECs encoding msFlt1 or AE+msFlt1 compared to controls (p=0.0608 and p=0.0287, respectively; Figure 5B–C).

Mice were also implanted with subcutaneous S2VP10 pancreatic cancer cells following the same procedure as described above (Figure 5D). In this experiment, tumor growth was slower in all treatment groups compared to controls (p-values for AE, hsFLT1, and AE +hsFLt1 were 0.0136, 0.0758, and 0.0655 respectively).

In vivo transgene expression of endostatin

To confirm the presence and sustainable production of transgene products, serum levels of murine endostatin were measured in mice implanted with Lewis lung carcinoma cells using an ELISA assay. Serum samples were collected at the end of the experiment described above from animals sacrificed on day 20 after the initiation of BOEC injections. The average endostatin levels in mice injected with AE-BOECs and AE+hsFlt-hBOECs were 441 ng/ml (range: 340–601 ng/ml) and 324 ng/ml (range: 260–342 ng/ml), respectively. These endostatin levels were both significantly higher than the levels in mice injected with DsRed-hBOECs (152 ng/ml; range: 96–190 ng/ml; p=0.01 and p=0.03, respectively).

Survival of mice with oncogene-induced brain tumor

Brain tumors were induced by injecting SV40-LgT and NRAS transposons into the right ventricle of 1-day-old C57BL/6 mice as detailed in the methods. Overall survival was calculated from date of injection to date of death or was censored at last date of follow-up for mice still alive at the end of the experiment. Median survival was 102.5 days (95% CI: 48–108 days) for mice treated with hsFlt1-mBOECs (n=10), 66 days (95% CI: 41–80 days) for control mice receiving no treatment (n=10), and 51 days (95% CI: 36–93 days) for the mice treated with wild-type mBOECs (n=7) (Figure 6). Survival differed significantly when testing all three groups (p=0.0453). Survival was significantly better in mice treated with hsFlt-1-mBOECs compared to mice receiving no treatment (p=0.0130) and was borderline

significantly better in mice treated with hsFlt-1-mBOECs compared to mice treated with wild-type BOECs (p=0.0871).

Discussion

The present study demonstrates that BOEC infusions can be effectively used for the local delivery of angiogenic inhibitors to primary tumor and metastatic foci in a wide variety of solid tumors. Wei et al. have reported that BOECs are selectively attracted to different primary tumors or metastases in particular organs. (14) One explanation for this preferential attraction is that tumors and inflammatory cells residing within tumors secrete different levels of angiogenic growth factors, with VEGF possibly being the primary chemoattractant for BOEC homing, though other factors may be involved such as placental growth factor and basic fibroblast growth factor. (15, 16) However, little is known about the mechanism by which circulating endothelial cells (17, 18) migrate to ischemic or cancerous tissue, with even less being known about the mechanism(s) attracting BOECs to pathologic tissue.

In the present study, we observed tumor responses to BOEC-mediated angiogenic inhibition that are consistent with what is known about the pathophysiology of these tumors. BOECs expressing sFlt1 had a profound effect on the survival of mice with gliomas, which are abundantly vascularized tumors dependent on the VEGF pathway. (19) In our pancreatic cancer model, single-agent treatment with BOECs expressing AE or sFlt inhibited tumor growth, but their combination did not result in an additive effect, possibly because VEGF inhibition is sufficient to achieve a maximal effect on angiogenic inhibition. Thus, addition of AE would not be expected to further improve the efficacy of this antiangiogenic strategy. However, the treatment of Lewis lung carcinoma tumors with BOECs expressing AE and BOECs expressing sFlt did result in improved inhibition compared to single-agent treatment. In this tumor model, angiogenic growth may be dependent on different growth factors; thus, the use of only one type of angiogenic inhibitor would be insufficient to impede tumor vascularization. We hypothesize that these differences among tumor types are likely due to different levels of dependency on the VEGF pathway.

When evaluating the clinical implications of an antiangiogenic BOEC, it is important to understand the impact of the transgene product on BOEC proliferation. Although non-transduced BOECs grow at a very fast pace in culture, their proliferation *in vitro* is negatively impacted by both the AE and sFlt1 proteins in suboptimal culture conditions. The addition of endothelial growth factors and serum to the culture medium overrides the inhibitory effect of the transgene product. Thus, sFlt, AE, and DsRed BOECs are capable of growing in culture, albeit at a somewhat slower pace, and providing an ample supply of cells for gene transfer. Although genetically modified BOECs can proliferate in vitro, it is still unknown how well they will proliferate in vivo in the hypoxic condition of growing tumor. Future studies will closely evaluate the effect of antiangiogenic transgenes on BOEC proliferation in vivo.

A suicide gene strategy has also been developed using transfused BOECs armed with a cytosine deaminase/uracil phosphoriosyltransferase fusion gene. (14, 20) Our previous work has shown that BOECs integrate into tumor vessels at very low levels (5 BOECs/100,000

tumor cells). (5) As a result, long-term cell survival is an important aspect to consider when designing BOEC-mediated therapies. Unlike a suicide gene strategy, an antiangiogenic strategy allows for the constant production of angiogenic inhibitors by BOECs. In the present study, sustainable levels of endostatin were detected in the serum of animals 24 days after the last BOEC infusion. These data are consistent with our *in vitro* data. Transgene expression was maintained for as long as it was tested (several months) in culture and over several cell passages and freezing/re-thawing cycles. Thus, an antiangiogenic strategy is capable of delivering a continuous therapeutic effect. In addition, an antiangiogenic strategy is less dependent on the degree of endothelial cell integration into the tumor vasculature.

Another important question that remains unanswered is whether non-transduced BOECs accumulate, migrate, preferentially survive, or proliferate in the tumor vasculature *in vivo*. We and others have previously reported that intravenously infused BOECs are initially found in the lung, liver, spleen, and tumor but at later time points preferentially survive in the tumor vasculature and augment vessel growth through incorporation into the vessel endothelium. (5, 14, 21) A shortcoming of previous studies is that the distribution of BOECs was only tracked for short periods of time. The present study tracked the number of BOECs in tumor tissue and other organs for 15 days after BOEC infusion. A large number of BOECs lodged in the pulmonary vasculature during their initial passage through the vascular network at 3 hours. Although the number of BOECs in other organs remained relatively stable at days 9 and 15, the number of BOECs in tumor tissue increased from day 9 to day 15. If migration or accumulation were responsible for an increase in BOECs in tumor tissue, then one would expect the number of BOECs in other organs to decrease correspondingly. Because this was not observed, it is reasonable to tentatively conclude that BOECs are capable of surviving and proliferating in the tumor microenvironment. Additional preclinical studies of genetically modified BOECs will need to provide mechanistic evidence of BOEC proliferation in tumor tissue, quantify the degree of proliferation, and determine organ selectivity before this method of gene therapy delivery can be applied to the clinic.

The safety of using BOEC-mediated gene therapy is also an important concern with respect to both the BOEC itself and the biological effects of the transgene product. In our glioma model, even though the median survival of mice treated with BOECs encoding human Flt1 was 102.5 days, the median survival of mice treated with wild-type BOECs was 51 days compared to 66 days for mice receiving no treatment ($p=0.6499$). This finding may raise the concern that BOECs might promote tumor angiogenesis and facilitate tumor growth or spread, thus negatively affecting survival. Clinical applications may have to use rigorous techniques for producing pure populations of therapeutic BOECs that are not contaminated with wild-type BOECs. By using antibiotic selection, we have been able to prevent contamination with unmodified BOECs and establish pure populations of BOECs expressing antiangiogenic transgenes. Animals infused with pure populations of therapeutic BOECs have not exhibited any negative side effects on weight or behavior in our studies. Although additional safety evaluations will need to be performed in larger animals, our findings support the continued development of BOECs as a cellular vehicle for therapeutic gene transfer in an autologous setting.

Acknowledgments

We thank The Susan G. Komen Breast Cancer Foundation (Grant # BCTR86006)(AZD) for supporting this research. This work was also supported by grants from the NIH; HL-55552 (RPH), CA109582 (KG), NS055738-01A2 (JRO), and the Dana Foundation (JRO). We thank Julia Nguyen from the Department of Medicine, University of Minnesota for culture and immunophenotyping of blood outgrowth endothelial cells, and Michael J Franklin from the University of Minnesota for editorial review.

References

1. Folkman J. Tumor angiogenesis: therapeutic implications. N Engl J Med. 1971 Nov 18; 285(21): 1182–6. [PubMed: 4938153]
2. Asahara T, Masuda H, Takahashi T, Kalka C, Pastore C, Silver M, et al. Bone marrow origin of endothelial progenitor cells responsible for postnatal vasculogenesis in physiological and pathological neovascularization. Circ Res. 1999 Aug 6; 85(3):221–8. [PubMed: 10436164]
3. Lin Y, Weisdorf DJ, Solovey A, Hebbel RP. Origins of circulating endothelial cells and endothelial outgrowth from blood. J Clin Invest. 2000 Jan; 105(1):71–7. [PubMed: 10619863]
4. Lin Y, Chang L, Solovey A, Healey JF, Lollar P, Hebbel RP. Use of blood outgrowth endothelial cells for gene therapy for hemophilia A. Blood. 2002 Jan 15; 99(2):457–62. [PubMed: 11781225]
5. Dudek AZ, Bodempudi V, Welsh BW, Jasinski P, Griffin RJ, Milbauer L, et al. Systemic inhibition of tumour angiogenesis by endothelial cell-based gene therapy. Br J Cancer. 2007 Aug 20; 97(4): 513–22. [PubMed: 17653078]
6. Ohlfest JR, Demorest ZL, Motooka Y, Vengco I, Oh S, Chen E, et al. Combinatorial antiangiogenic gene therapy by nonviral gene transfer using the sleeping beauty transposon causes tumor regression and improves survival in mice bearing intracranial human glioblastoma. Mol Ther. 2005 Nov; 12(5): 778–88. [PubMed: 16150649]
7. Somani A, Nguyen J, Milbauer LC, Solovey A, Sajja S, Hebbel RP. The establishment of murine blood outgrowth endothelial cells and observations relevant to gene therapy. Transl Res. 2007 Jul; 150(1):30–9. [PubMed: 17585861]
8. Maroulakou IG, Anver M, Garrett L, Green JE. Prostate and mammary adenocarcinoma in transgenic mice carrying a rat C3(1) simian virus 40 large tumor antigen fusion gene. Proc Natl Acad Sci U S A. 1994 Nov 8; 91(23):11236–40. [PubMed: 7972041]
9. Yoshino H, Ueda T, Kawahata M, Kobayashi K, Ebihara Y, Manabe A, et al. Natural killer cell depletion by anti-asialo GM1 antiserum treatment enhances human hematopoietic stem cell engraftment in NOD/Shi-scid mice. Bone Marrow Transplant. 2000 Dec; 26(11):1211–6. [PubMed: 11149733]
10. Weidner N, Semple JP, Welch WR, Folkman J. Tumor angiogenesis and metastasis--correlation in invasive breast carcinoma. N Engl J Med. 1991 Jan 3; 324(1):1–8. [PubMed: 1701519]
11. Wiesner SM, Decker SA, Larson JD, Ericson K, Forster C, Gallardo JL, et al. De novo induction of genetically engineered brain tumors in mice using plasmid DNA. Cancer Res. 2009 Jan 15; 69(2): 431–9. [PubMed: 19147555]
12. Zhou XH, Gao S. Confidence intervals for the log-normal mean. Stat Med. 1997 Apr 15; 16(7): 783–90. [PubMed: 9131765]
13. Kaplan ELMP. Nonparametric Estimation from Incomplete Observations. Journal of the American Statistical Association. 1958; 53(282):457–81.
14. Wei J, Jarmy G, Genuneit J, Debatin KM, Beltinger C. Human blood late outgrowth endothelial cells for gene therapy of cancer: determinants of efficacy. Gene Ther. 2007 Feb; 14(4):344–56. [PubMed: 17024106]
15. Ferrari N, Glod J, Lee J, Kobiler D, Fine HA. Bone marrow-derived, endothelial progenitor-like cells as angiogenesis-selective gene-targeting vectors. Gene Ther. 2003 Apr; 10(8):647–56. [PubMed: 12692593]
16. Autiero M, Luttun A, Tjwa M, Carmeliet P. Placental growth factor and its receptor, vascular endothelial growth factor receptor-1: novel targets for stimulation of ischemic tissue revascularization and inhibition of angiogenic and inflammatory disorders. J Thromb Haemost. 2003 Jul; 1(7):1356–70. [PubMed: 12871269]

17. Hristov M, Weber C. Endothelial progenitor cells: characterization, pathophysiology, and possible clinical relevance. J Cell Mol Med. 2004 Oct-Dec;8(4):498–508. [PubMed: 15601578]

18. Li X, Tjwa M, Moons L, Fons P, Noel A, Ny A, et al. Revascularization of ischemic tissues by PDGF-CC via effects on endothelial cells and their progenitors. J Clin Invest. 2005 Jan; 115(1): 118–27. [PubMed: 15630451]

19. Benjamin LE, Golijanin D, Itin A, Pode D, Keshet E. Selective ablation of immature blood vessels in established human tumors follows vascular endothelial growth factor withdrawal. J Clin Invest. 1999 Jan; 103(2):159–65. [PubMed: 9916127]

20. Wei J, Blum S, Unger M, Jarmy G, Lamparter M, Geishauser A, et al. Embryonic endothelial progenitor cells armed with a suicide gene target hypoxic lung metastases after intravenous delivery. Cancer Cell. 2004 May; 5(5):477–88. [PubMed: 15144955]

21. Milbauer LC, Enenstein JA, Roney M, Solovey A, Bodempudi V, Nichols TC, et al. Blood outgrowth endothelial cell migration and trapping in vivo: a window into gene therapy. Transl Res. 2009 Apr; 153(4):179–89. [PubMed: 19304277]

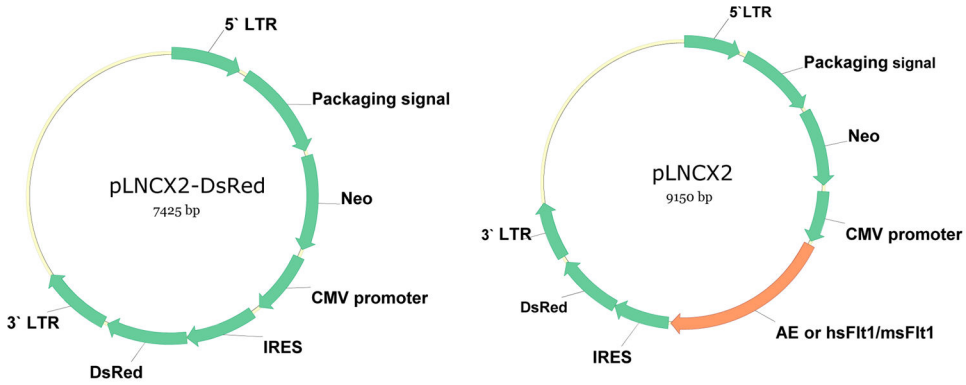

Figure 1.
Retroviral vectors expressing anti-angiogenesis gene.

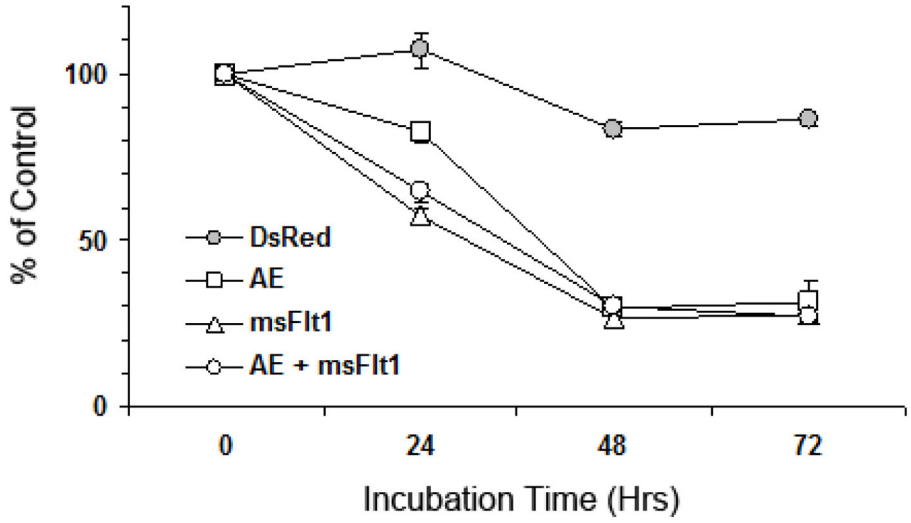

Figure 2.

Inhibition of endothelial cell proliferation *in vitro*. A proliferation assay was performed on PVECs exposed to conditioned medium from transduced BOECs expressing angiostatin and endostatin (AE), mouse soluble Flt-1 receptor (msFlt1) or DsRed or a medium from a mixed BOEC culture (AE+msFlt1). Results are relative to PVECs cultured with basal medium supplemented with CAMP and FGF. Data points represent the means ± S.E. of six wells from one experiment.

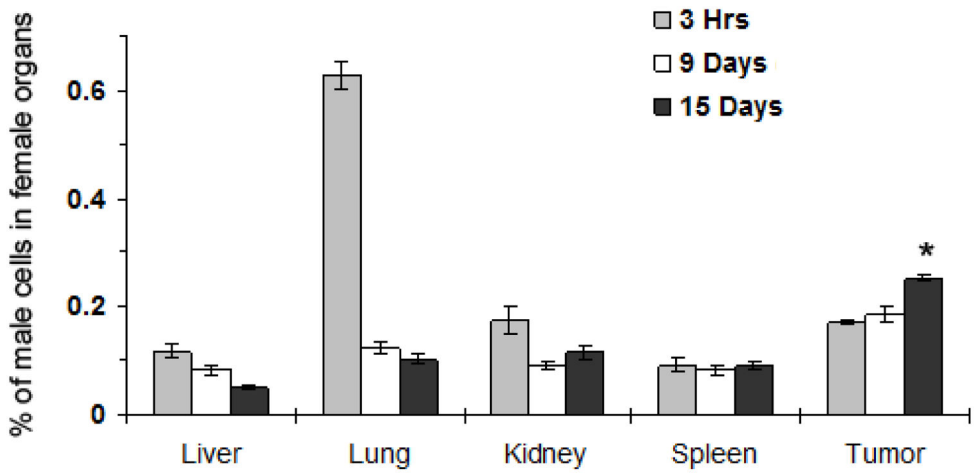

Figure 3.

Distribution of male BOECs (mBOECs) in the organs of female mice. Indicated organs were harvested from mice at 3hrs (n=10), 9 days (n=15) and 15 days (n=15) after mBOEC injections. Genomic DNA in each organ was analyzed by real-time quantitative PCR for Y chromosome-specific DNA sequences. Data points represent the means ± S.E. * indicates a significant difference in the number of BOECs in the tumor on day 9 versus day 15 ($P<0.0001$), significant difference in the number of BOECs in tumor tissue versus lung ($p<0.0001$), and a decrease in the number of BOECs in the liver ($p=0.0042$)

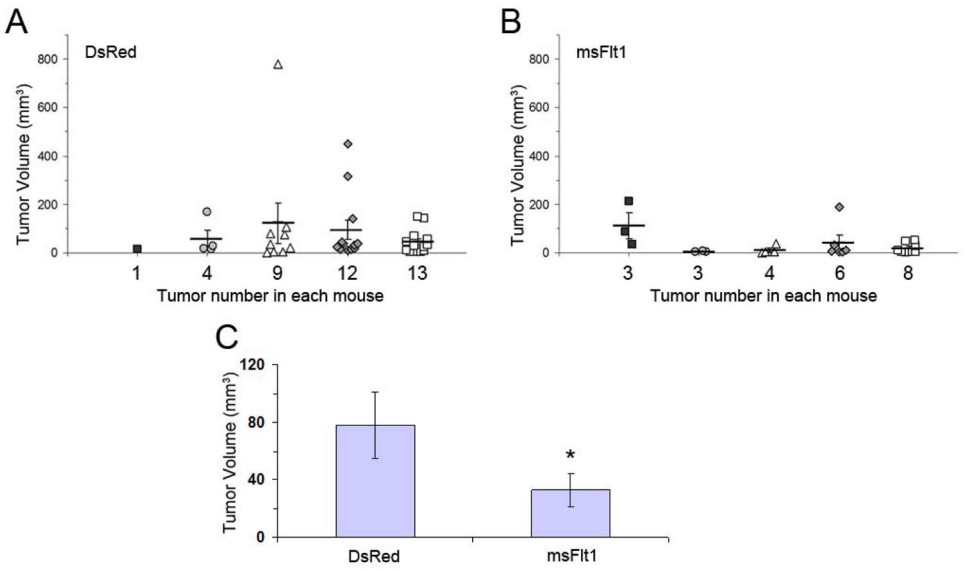

Figure 4.

Mouse BOECs encoding msFlt1 suppress spontaneous tumor growth. Mice bearing spontaneous mammary tumors were sacrificed 9 days after i.v. injection with DsRed-BOECs (n=5) or msFlt1-BOECs (n=5). (A, B) Tumor size and number of metastases. Each column represents data from an individual animal, and numbers along the x axis indicate the total number of tumors observed in each animal. Individual tumors, average tumor volume, and SE for each mouse are shown. Mice receiving msFlt1-mBOECs had smaller primary and fewer metastatic tumors on day 9 than mice receiving DsRed-mBOECs (p=0.0613). (C) Average tumor volume. * indicates a significant difference in average tumor volume (p=0.0095). Error bars represent 95% CI.

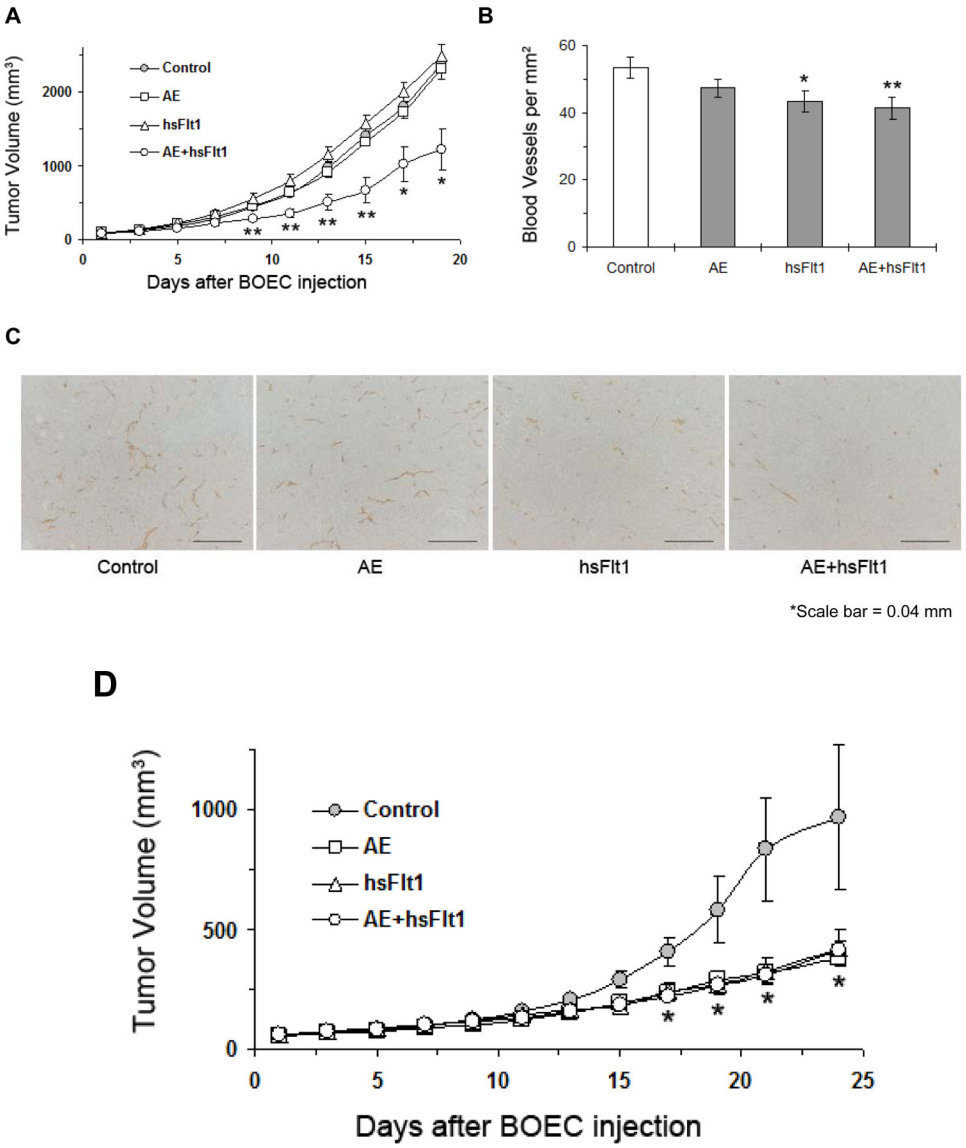

Figure 5.

BOEC gene delivery of AE and sFlt1 suppress established tumor growth and tumor vascular growth. (A) Lewis lung carcinoma tumor growth curve after BOEC treatment. Day 0 represents the last (third) injection of BOECs and day 8 after subcutaneous tumor implantation. An anti-asialo GM1 antibody was used to eliminate NK cells before mice were treated with 1.5×10^6 cells of BOECs by i.v. injection. * indicates a significant difference in tumor volume between AE+hsFlt1-hBOECs and all other groups ($p \leq 0.001$). n=10 per group. (B, C). Blood vessel density in Lewis lung carcinoma tumors. Tumor tissue was collected from control mice (n=5) and each treatment group (n=4 per group). Tissue sections were stained for CD31. Microvessels were counted in 5–11 random 0.0321-mm^2 fields taken of each section at 200× magnification. (B) Immunohistochemical data were quantified. **$p<0.05$, *$p<0.10$ vs BOEC control. (C) Representative sections are shown illustrating the differences in vessel density as detected with CD31. (D) S2VP10 tumor growth curve after

BOEC treatment. The same procedure as described above was applied. * indicates a significant difference in tumor volume between AE-BOECs and control DsRed-BOECs (n=10 per group; p= 0.0136).

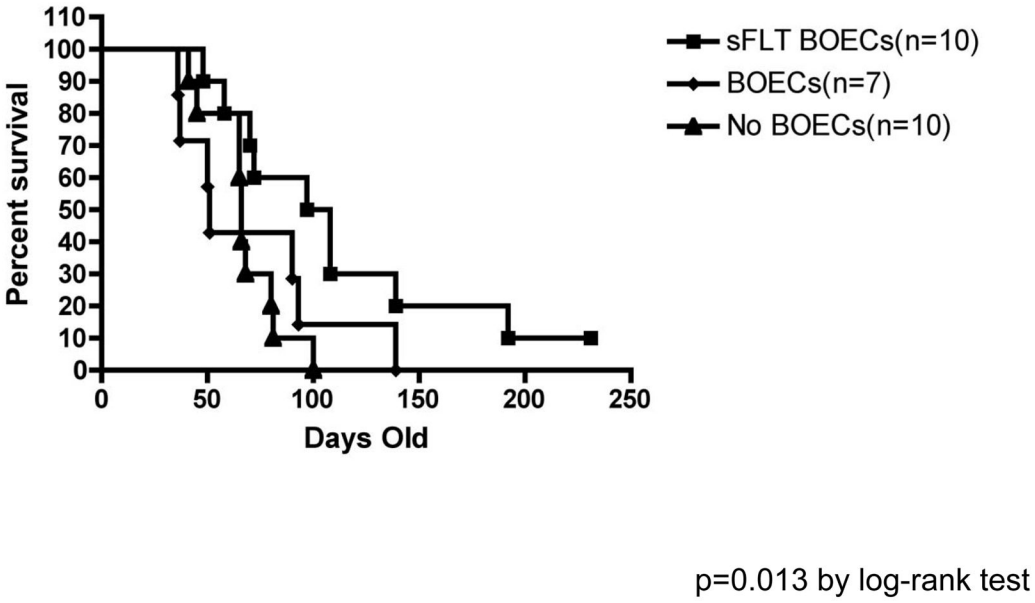

Figure 6.

Kaplan Meier survival curves for mice with spontaneous malignant glioma receiving no treatment (n=10), wild-type murine BOECs (n=7), or murine BOECs encoding hsFlt1 (sFlt1-BOEC) (n=10). A significant difference was seen between mice treated with hsFlt-1-mBOECs compared to mice receiving no treatment (p=0.0130), whereas a borderline significant difference was seen for mice treated with hsFlt-1-mBOECs compared to mice treated with wild-type BOECs (p=0.0871).